DEVELOPMENT OF AMORPHOUS SOLID DISPERSION TABLET OF SORAFENIB WITH IMPROVED ORAL BIOAVAILABILITY

A THESIS

SUBMITTED TO THE FACULTY OF THE

UNIVERSITY OF MINNESOTA BY

Sichen Song

IN PARTIAL FULFILLMENT OF THE REQUIREMENTS

FOR THE DEGREEE OF MASTER OF SCIENCE

Thesis Advisor: Ronald A. Siegel, Sc.D.

May 2021

Acknowledgements

First, I would like to thank my advisor, Dr. Ronald Siegel, for his continuous support, patience, and encouragement of my education and research, and for his astounding broad knowledge in multiple disciplines. I could not imagine having a better advisor, for my research and personal growth.

I would also like to thank my thesis defense committee members: Dr. Changquan Calvin Sun and Dr. Chun Wang, for their careful review and valuable feedback of the thesis.

In league with Dr. Siegel, I thank Dr. Changquan Calvin Sun, for his cosupervision of this work. His professional insights and broad knowledge in pharmaceutical material science and engineering is equally impactful to my professional growth.

I would also like to express my deepest gratitude to Dr. Chenguang Wang, with whom I worked and learnt a lot in solid-state pharmaceutics in the past couple of years. His insight and guidance in my work is highly appreciated.

I would like to extend my sincere thanks to other skilled and patient individuals, including Dr. Timothy Lodge, for his kindness to allow me to access to his mini spray dryer; Nicholas Van Zee and Monica Ohnsorg, for their training and assistance in spray drying; Dr. Shan Wang, for his assistance in the particle dissolution study; Gerrit Vreeman, for collecting SEM images; Wenjuan Zhang, Dr. William Elmquist and Dr. Ronald

Sawchuk, for their helpful interpretations and discussions of the PK study; Dr. Timothy Wiedmann, for his careful review and valuable comments on my manuscript.

I would like to express my appreciation to my parents and Wenjuan, for their company, encouragement, and unconditional love.

Finally, funding from Huadong Medicine Co., Ltd. is acknowledged.

Dedication

To my parents and Wenjuan

Abstract

An amorphous solid dispersion (ASD) immediate release tablet of sorafenib (SOR) was developed to improve oral bioavailability. The ASD was produced by coprecipitating both SOR and an enteric polymer, hydroxypropyl methylcellulose acetate succinate (HPMC-AS). The goal of maintaining supersaturation of ASDs was used to guide the selection of drug loading and HPMC-AS grade. The ASD of 40% drug loading with HPMC-AS M grade, which exhibits superior physical stability, enhanced dissolution extent and moderate hygroscopicity, was selected for further tablet development. Tablet formulation composition and dry granulation process were designed to achieve fast disintegration and adequate flow properties, and to mitigate over-granulation that would compromise *in vivo* performance. A material sparing and expedited approach was used to optimize compaction pressure to manufacture the ASD tablet with low friability and rapid disintegration. The resulting SOR ASD tablet showed enhanced *in vitro* dissolution rate and extent compared to the marketed product Nexavar®. A pharmacokinetic study in dogs suggested that the SOR ASD tablet exhibited a 1.5-fold improvement in the relative oral bioavailability compared to Nexavar®.

Graphical Abstract

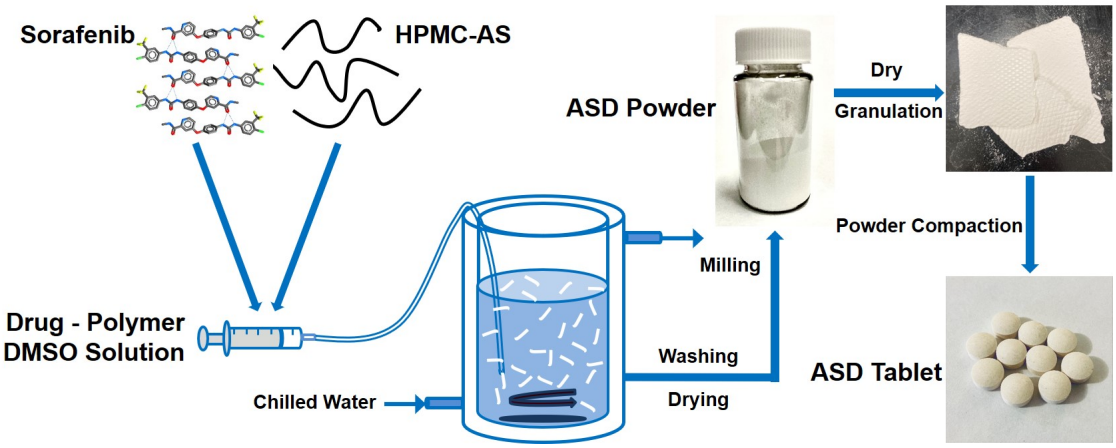

Table of contents

List of Tables

List of Figures

1. Introduction

In recent decades, advances in automated organic synthesis, combinatorial chemistry, innovative high-throughput screening, and rational drug design have led to the production of a large number of marketed drug and potential drug candidates. These molecules often have poor aqueous solubility, which significantly limits their oral bioavailability.[1] According to the Biopharmaceutics Classification System (BCS), drugs are classified into four categories based on solubility and membrane permeability.[2] For BCS II drugs with good permeability but poor aqueous solubility, formulation strategies play a critical role in improving their oral bioavailability. Among those solubilization-enhancing strategies, amorphous solid dispersion (ASD) has been shown to be an effective technique to increase oral bioavailability of BCS II drugs.[3-5]

The two prevalent large scale processing methods to prepare ASDs are spray drying and hot melt extrusion (HME). Spray drying is a solvent mediated method, which requires drug and polymer dissolution in a low boiling point solvent with low viscosity.[6] HME, on the other hand, is a solvent free manufacturing process. Drug and polymer are heated and mixed at approximately 20-30 °C above the melting temperature of the drug, and then rapidly quenched.[7] However, drugs with poor solubility in low boiling point solvents and high melting temperature are not amenable for these two ASD processing methods. For example, vemurafenib, a poorly water-soluble drug, has low solubility in commonly used volatile solvents including methanol, acetonitrile, dichloromethane, isopropanol, and acetone. It also exhibits an extremely high melting temperature,

272.1 °C.[8] To produce ASDs of such compounds, a coprecipitation method has been introduced.[8-10]

The coprecipitation method combines drug and polymer in a solvent to generate ASD when dispersed in an aqueous antisolvent. Physicochemical properties of desirable drug candidates for coprecipitation include high lipophilicity, limited aqueous solubility, and low crystallization tendency in the antisolvent. Polymers are limited to ionic polymers, such as hypromellose phthalate, hydroxypropyl methylcellulose acetate succinate (HPMC-AS), and polymethacrylates (different grades of Eudragit®), since they are insoluble in aqueous antisolvent when pH is suitably adjusted. A high concentration drug/polymer stock solution is introduced into chilled aqueous media either drop wise or by nozzle spraying, in batch mode, or by pumping streams of stock solution and aqueous media into a chamber with a high-shear mixer under continuous mode. The drug/polymer solution is dispersed as small droplets into the antisolvent with high-speed shearing, and the solvent rapidly diffuses out simultaneously with water diffusion into the droplets. Precipitation can occur when drug concentration exceeds its amorphous solubility. Coprecipitates containing residual solvent and antisolvent are then collected from the suspension by vacuum filtration or centrifugation in batch mode, or they are pumped into the next unit of isolation using a centrifugal filter under continuous manufacturing. After washing in antisolvent and deionized (DI) water to remove residual solvent and acidic or basic components, the hydrated coprecipitate is dried using a fluid bed dryer, balancing the demands of moderate drying temperature and short drying time. The fresh ASD is then milled to reduce particle size by jet or ball milling. Granulation is always necessary because the ASD exhibits low bulk density and poor flowability.[9]

Using the process described above, vemurafenib, which is unsuitable for spray drying and HME, was coprecipitated with HPMC-AS as a homogeneous ASD, and has been commercialized successfully under the trade name Zelboraf®.[8] Although coprecipitation is a highly complex process with numerous unit operations, a high throughput miniaturized coprecipitation screening (MiCoS) has been established to facilitate rapid optimization of critical processing parameters and to assess the performance of ASDs on a milligram scale.[8]

Sorafenib (SOR), a drug used to treat hepatocellular carcinoma,[11,12] has a very low solubility of approximately 10 ng/mL in 50 mM pH 6.8 phosphate-buffered saline (PBS) at room temperature.[13] It is classified as a BCS II drug due to its relatively high membrane permeability and large dose/solubility ratio.[14] The marketed product Nexavar® contains the tosylate salt of SOR, and the relative oral bioavailability is only 38-49% compared with oral solution in the fasted state.[14] Several formulation strategies to enhance the oral bioavailability and efficacy of SOR have been reported, including nanocomplexes with ionic liquids, nanoparticles, suspensions, self-microemulsifying drug delivery systems, capsules containing Eudragit® ASD, and physical mixture with polyvinylpyrrolidone/vinyl acetate (PVP-VA).[14-20]

To address the low oral bioavailability of Nexavar®, we have developed an SOR ASD tablet formulation to enhance dissolution and oral bioavailability. We demonstrate that the material sparing and expedited approach is a robust method to design the ASD tablet with several advantages including high-speed tableting, rapid disintegration time, low friability and enhanced *in intro* and *in vivo* performance.

2. Materials and Methods

2.1 Materials

SOR free base (**Figure 1A** and **Table 1**) and tosylate salt (Huadong Medicine Co., Ltd., Hangzhou, China), HPMC-AS (AquaSolve™ M/L/HF; Ashland, Wilmington, DE **Figure 1B**), microcrystalline cellulose (Avicel® DG and PH-102; FMC Biopolymers, Newark, DE), D-(-)-tartaric acid (Sigma-Aldrich, St. Louis, MO), crospovidone (Kollidon® CL-SF; BASF, Ludwigshafen, Germany), magnesium stearate (MgSt; Mallinckrodt Inc., St. Louis, MO), dimethyl sulfoxide (DMSO; Fisher Scientific, Fair Lawn, NJ), hydrochloric acid aqueous solution (HCl, 36.5% - 38%; VWR International LLC., Radnor, PA), sodium phosphate dibasic heptahydrate and sodium phosphate monobasic monohydrate ($Na_2HPO_4 \cdot 7H_2O$, $NaH_2PO_4 \cdot H_2O$; Fisher Scientific, Fair Lawn, NJ), polysorbate 80 (Tween® 80; VWR Life Science, manufactured by AMRESCO LLC., Solon, OH), sodium lauryl sulfate (Kolliphor® SLS; BASF, Ludwigshafen, Germany), ethanol (VWR International LLC., Radnor, PA), methanol (MeOH; Sigma-Aldrich, St. Louis, MO) and dichloromethane (DCM; Sigma-Aldrich, St. Louis, MO), were all used as received.

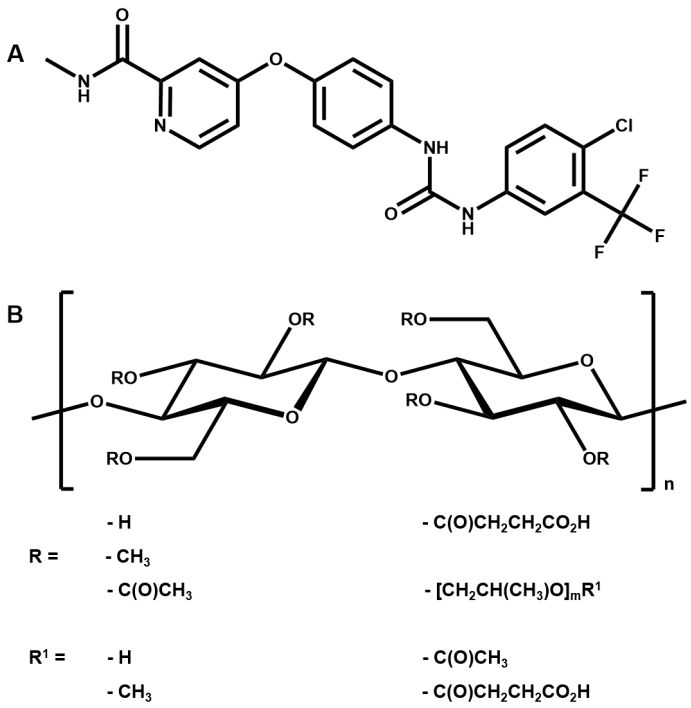

Figure 1. Chemical structure of A) SOR free base, B) HPMC-AS.

Table 1. Physicochemical properties of SOR free base.

Compound property	Value
Molecular formula	$C_{21}H_{16}ClF_3N_4O_3$
Molecular Weight (g/mol)	464.825
pKa	11.55, 2.03[a]
LogP	3.8
T_g (°C)	~88
T_m (°C)	~212
Crystalline solubility (µg/mL)[b]	9.86×10^{-3} [13]
Amorphous solubility (µg/mL)[b]	0.53 - 0.64 [13]
Supersaturation ratio[b]	54.0 - 64.5 [13]

[a] Predicted using ChemAxon prediction tool. [b] Measured in 50 mM pH 6.8 PBS.

2.2 Methods

2.2.1 Preparation of SOR/HPMC-AS ASDs by the coprecipitation method

SOR/HPMC-AS (M) ASDs were prepared by coprecipitation. First, 1.2 g of SOR and 1.8 g HPMC-AS mixture was dissolved in 20 mL DMSO. The SOR/HPMC-AS DMSO solution was then dispersed in 200 mL 0.01 N HCl antisolvent in a water-jacketed beaker with temperature maintained at 4 °C and stirred at 800 rpm with magnetic stirring, using a syringe pump with flow rate 5 mL/min, to obtain the coprecipitate (**Figure 2**). The coprecipitate was collected by vacuum filtration and washed three times with 200 mL 0.01 N HCl to remove residual DMSO and then three times with DI water to remove residual DMSO and HCl. Finally, the precipitate was vacuum dried for 24 hr to remove residual water. SOR/HPMC-AS (L/H) ASDs with 40% drug loading and SOR/HPMC-AS (M) ASDs with 20% and 60% drug loadings were prepared by the same method. Received ASDs were milled manually using a mortar and pestle to reduce particle size.

2.2.2 Preparation of amorphous SOR tosylate and SOR tosylate/HPMC-AS ASD by spray drying

Amorphous SOR tosylate and SOR tosylate/HPMC-AS ASD were prepared by spray drying 2 wt % solution in DCM/MeOH (50:50, v/v) using a mini spray dryer (Bend Research). Briefly, 300 mg of powder was dissolved in 18 mL of cosolvent. The solution was transferred to a 20 mL syringe and injected into the spray dryer. The inlet temperature was 80 °C, and the outlet temperature was approximately 25 °C. Solution flow rate was 0.65 mL/min, and nitrogen gas flow rate was 12.8 standard liters per minute (SLPM). The spray dried samples were collected on filter paper, transferred into scintillation vials, and

vacuum dried at ambient temperature for at least 24 hrs to remove all residual solvents before further use.

2.2.3 Powder X-ray diffraction (PXRD)

Powder X-ray diffractograms were obtained using a laboratory X-ray diffractometer (D8 Advance; Bruker AXS, Madison, WI) with Cu Kα radiation (1.54059 Å). Samples were scanned between 5° and 35° 2θ with a step size of 0.019699° at 1 s/step and a dwell time of 0.5 s. Tube voltage and amperage were set at 40 kV and 40 mA, respectively.

2.2.4 Thermal analysis

Powders (~3 mg) were loaded into Tzero hermetically sealed aluminum pans and heated at 10 °C/min from room temperature to ~230 °C in a differential scanning calorimeter (Q1000; TA Instruments, New Castle, DE) under continuous nitrogen purge at a flow rate of 25 mL/min.

2.2.5 Moisture sorption isotherms

Water sorption isotherms of samples were obtained using an automated vapor sorption analyzer (Intrinsic DVS, Surface Measurement Systems Ltd., Allentown, PA) at 25 °C. The nitrogen flow rate was 50 mL/min. Each sample was first dried with a nitrogen purge until a constant weight was obtained. The sample was then exposed to relative humidities (RH) ranging from 0% to 95% in 5% increments. At each RH, the equilibration criterion of either $dm/dt \leq 0.002\%$/min, with a minimum equilibration time of 0.5 hr or maximum equilibration time of 6 hr, was applied.

2.2.6 Polarized light microscopy (PLM)

Images of samples were recorded with a PLM (Eclipse E200; Nikon, Tokyo, Japan).

2.2.7 Scanning electron microscopy (SEM)

Samples were mounted onto carbon tape-covered SEM stubs and sputter coated with a thin layer of platinum (thickness ~50 Å) using an ion beam sputtering system (IBS/TM200S; VCR Group Inc., San Clemente, CA). Surface features of the ASD and tablet were imaged using SEM with an FEI Helios NanoLab G4 dual beam focused ion beam instrument operated in field free mode with an Everhart Thornley detector, an acceleration voltage of 2 kV, and a current of 25 pA. The working distance was set around 4 mm. A high vacuum ($10^{-4} - 10^{-5}$ Pa) was maintained during the imaging process.

2.2.8 Nuclear magnetic resonance (NMR)

All ^{1}H NMR spectra were recorded on a Varian 400 MHz spectrometer, referenced to residual DMSO-d_6 (2.50 ppm).

2.2.9 Bulk powder dissolution study for SOR ASDs

Briefly, degassed 100 mM pH 6.8 PBS containing 0.1% Tween® 80 was prepared as the dissolution medium. A volume of 50 mL medium was introduced into a beaker, and appropriate amounts of ASD (from ASDs with different drug loadings) were added to achieve a target drug concentration of 0.8 mg/mL. Dissolution tests were conducted at room temperature. At time points of 10, 30, 60, 120, and 240 min, aliquots of the medium (~1 mL) were filtered and diluted 50 fold with ethanol. Drug concentrations were determined by a UV-Vis spectrometer (DU® 530 UV−Vis spectrophotometer; Beckman

Coulter, Inc., Brea, CA) at λ = 264 nm by interpolation from the appropriate standard curve.

2.2.10 Intrinsic dissolution rate (IDR)

IDR was measured using the rotating disc method. Each powder was compressed at a force of 1000 lb, using a custom made stainless steel die, against a flat stainless steel disc for 1 min to prepare a pellet (round, 6.39 mm in diameter). The resulting pellet had a visually smooth surface that was coplanar with the surface of the die. While rotating at 300 rpm, the die was immersed in 300 mL of dissolution medium (degassed 100 mM pH 6.8 PBS containing 0.1% SLS) at 37 °C in a water-jacketed beaker. A UV−Vis fiberoptic probe (Ocean Optics, Dunedin, FL) was used to continuously monitor UV absorbance of the dissolution medium at λ = 264.695 nm, to obtain concentration-time profiles based on a concentration-absorbance standard curve constructed previously ($R^2 > 0.99$).

Table 2. Formulation of SOR ASD tablet.

Material	Function	Percentage (%)	Weight (mg)
SOR free base	API	25	100
HPMC-AS (M)	Polymer matrix	37.5	150
Avicel® DG	Dry binder	25	100
D-(-)-Tartaric Acid	Disintegration facilitator/ pH modifier	7	28
Crospovidone	Disintegrant	5	20
MgSt	Lubricant	0.5	2
Total	-	100	400

2.2.11 Dry granulation

The ASD was mixed in a bottle with all excipients except for MgSt (**Table 2**) using a mixer (Turbula; GlenMills Inc., Clifton, NJ) for 15 min at 49 rpm (batch size was ~5 g). Mixtures were compacted into simulated ribbons of ~500 mg using a compaction simulator (STYL'One Evo; Medelpharm, Beynost, France) equipped with a flat-faced 16×9 mm rectangle punch under a compaction force of 7 KN. The ribbons were then ground manually using a mortar and pestle, passed through a 500 μm sieve, and mixed with MgSt using the same mixer for 1 min to obtain granules. Compaction of formulated granules was performed in the same compaction simulator using concave tooling (10 mm in diameter) to produce biconvex round tablets under different compaction forces. The targeted weight of SOR ASD tablets was 400 mg.

2.2.12 Flowability and bulk density

Powder flowability for ASDs, pre-slugging mixtures, formulated granules with or without MgSt, Avicel® PH-102 and DG, were quantified under ambient conditions (23 ± 1 °C and 20 - 40% RH) using a ring shear cell tester (RST-XS; Dietmar Schulze, Wolfenbüttel, Germany) and a shear cell (XS-Mv4) with 9.65 mL volume under a pre-shear normal stress of 3 kPa. Powders were sheared under a series of progressively increasing normal stresses of 0.5, 1, 1.5, 2, 2.5, and back to 0.5 kPa to construct a yield locus. The unconfined yield strength (σ_c) and major principal stress (σ_1) were obtained from each yield locus by drawing Mohr's circles. The flow function coefficient (*ffc*) was calculated to quantify flowability using $ffc = \sigma_1 / \sigma_c$.[21] Bulk density was obtained by dividing the mass of powder filled in the shear cell by the shear cell volume.

2.2.13 Tabletability

Formulated granules (~220 mg) were compressed under different pressures (25 – 170 MPa) using another compaction simulator (Presster; Metropolitan Computing Company, East Hanover, NJ) to simulate a Korsch XL400 29-station tablet press. Dwell time was set at 10.3 ms, corresponding to a production speed of 74,800 tablets/hr, and flat round tooling (10 mm) was used. Tablet diametrical breaking force was measured under ambient conditions (24 °C and 41% RH) using a texture analyzer (TA-XT2i; Texture Technologies Corporation, Scarsdale, NY) with a speed of 0.01 mm/s, and tablet dimensions were assessed using a digital caliper. Tablet tensile strength (σ, MPa) was calculated using the equation, $\sigma = 2F / \pi Dh$, where F is breaking force (N), D is tablet diameter (mm), and h is tablet out-of-die thickness (mm).[22]

2.2.14 Friability

The tablet friability profile, representing tablet weight loss with a series of compaction forces, was determined using an expedited method.[23] Tablets produced under different compaction forces were individually coded and loaded into a friabilator (F-2; Pharma Alliance, London, UK) operating at 25 rpm for 4 min. Tablets were weighed before and after the test to calculate the percentage weight loss for individual tablets (% friability), which was plotted as a function of compaction force.

2.2.15 Disintegration time

Disintegration time of tablets was measured in degassed 900 mL 100 mM pH 6.8 PBS with 0.1% Tween® 80 at 37 ± 0.5°C using a disintegration tester (Guoming® BJ-1; Tianjin Guoming Medicinal Equipment Co., Ltd, Tianjin, China) operating at 30

cycles/min. Disintegration time of each tablet was recorded as the time at which all granules had passed through the wire mesh.

2.2.16 *In vitro* dissolution study

Drug dissolution was performed using a USP II apparatus (VanKel 7010, Varian Inc., Cary, NC) in 500 mL degassed 100 mM pH 6.8 PBS with 0.1% Tween® 80 for both SOR ASD and Nexavar® tablets. Temperature was maintained at 37 ± 0.5 °C, and paddle speed was 75 rpm. SOR ASD tablet prepared under 3 KN compaction force was placed in the vessel. Aliquots of the medium (~2 mL) were taken at different time points (10, 20, 30, 45, 60, and 90 min) and immediately replaced with fresh medium. Aliquots were filtered through a 0.45 μm membrane, and the concentration of SOR was determined by UV-Vis at λ = 264 nm using a calibration curve with appropriate background correction (R^2> 0.99).

2.2.17 *In vivo* pharmacokinetic (PK) study

The PK performance of SOR ASD and Nexavar® tablets was evaluated in male beagle dogs (~10 kg, Beijing Marshall Biotechnology Co. Ltd, Beijing, China) using a crossover design (n = 3) with one week washout between doses. Dogs were fasted overnight prior to each dosing session and were given food 4 hr after dosing. Oral administration of tablets was followed immediately by gavage with approximately 10 mL of reverse osmosis water. Blood samples (~1 mL) were taken from the jugular vein at 0.25, 0.5, 1, 1.5, 2, 4, 6, 8, and 24 hr after dosing. Blood samples were stored on ice in K_2-EDTA-containing vacutainer blood collection tubes. Samples were subsequently centrifuged at 2200g for 10 min at 2-8 °C, and plasma was isolated and stored at -80 °C until analysis by LC-MS/MS-18 (Triple Quad™ 6500+ LC-MS/MS System; AB SCIEX,

Framingham, MA). The PK study was performed in accordance with standards recommended by the Guide for Care and Use for Laboratory Animals (U.S. National Institutes of Health, Bethesda, MD) and was approved by the Institutional Animal Care and Use Committee (IACUC) of Medicilon Preclinical Research (Shanghai) LLC, Shanghai, China. All PK parameters were calculated using noncompartmental analysis modules in the U.S. Food and Drug Administration certified PK program Phoenix WinNonlin 8.3 (Certara USA, Inc., Princeton, NJ).

3. Results and Discussion

3.1 ASD manufacturing method selection

The applicability of spray drying and HME for SOR ASD manufacturing was explored. Spray drying was found to be unsuitable due to poor solubility of SOR in volatile solvents. Because of the high melting temperature and poor thermal stability of SOR (**Figure 2**), HME was also excluded.

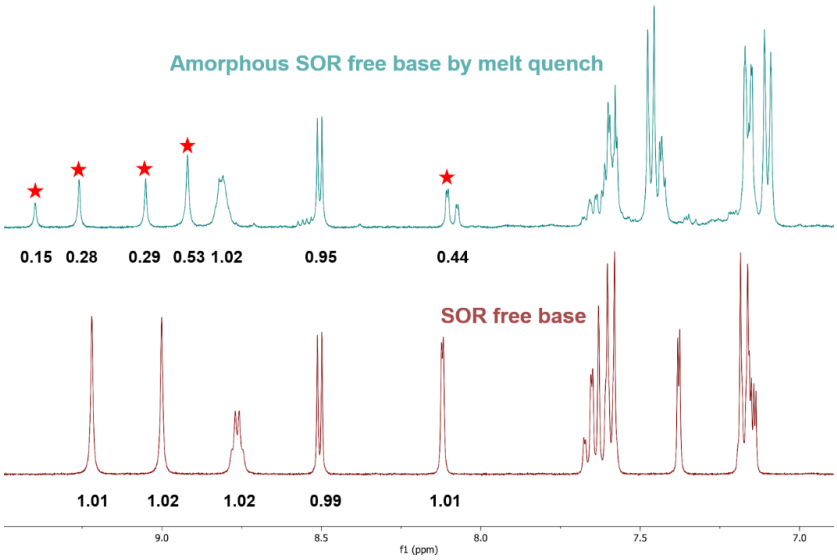

Figure 2. ^{1}H NMR of amorphous SOR free base by melt quench and SOR free base as received.

Figure 3 is a schematic diagram of the coprecipitation process used. DMSO was selected as solvent due to its ability to dissolve highly concentrated SOR/HPMC-AS mixtures, miscibility with aqueous antisolvent (acidic water), and low toxicity (ICHQ3 Guideline 2009). The aqueous media was adjusted to pH 2 to guarantee effective coprecipitation of SOR (acidic pK_a = 2.03) and HPMC-AS. The low temperature could further decrease the rate of nucleation and crystal growth as well as counter the heat

generated by continuous stirring.[9] After coprecipitation was complete, a washing process using both acidic and DI water was required, since precipitates contained DMSO and HCl. Unlike spray drying and HME, coprecipitation at the laboratory scale did not require any specialized apparatus. The yield was 75-80% (n = 3) after drying, indicating that coprecipitation is an efficient processing method.[20]

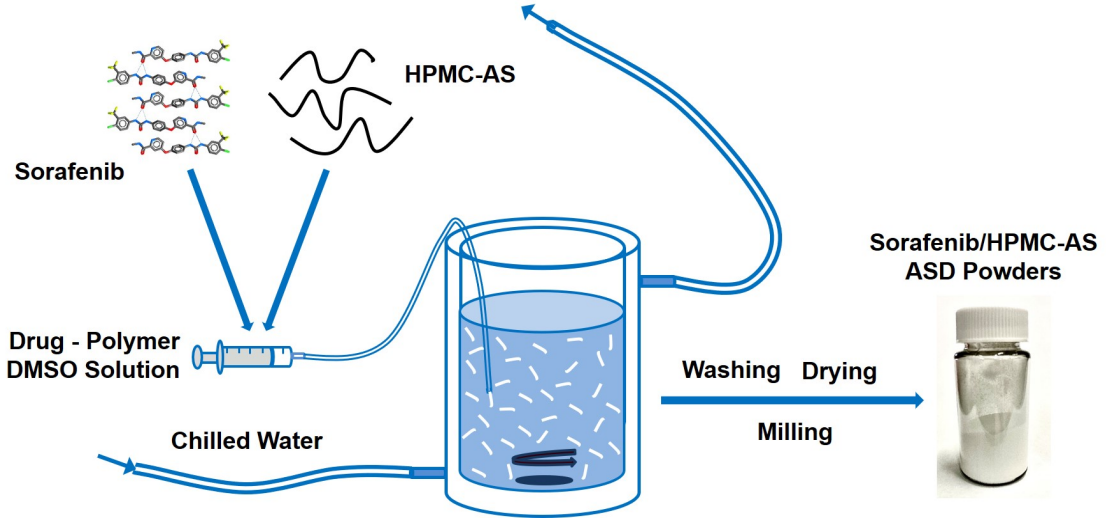

Figure 3. Scheme of the coprecipitation process.

SOR is a feasible candidate for coprecipitation for the following reasons: (1) its acidic pK_a was higher than the pH of the antisolvent, which minimized the degree of ionization and dissolution during precipitation; (2) it is a slow crystallizer in aqueous media (**Figure 4**); (3) SOR and HPMC-AS coprecipitated in a homogeneous amorphous form, because the polymeric stabilizer is also insoluble in acidic environment, and (4) both SOR, logP of 3.8, and polymer can form favorable hydrophobic interactions.[24]

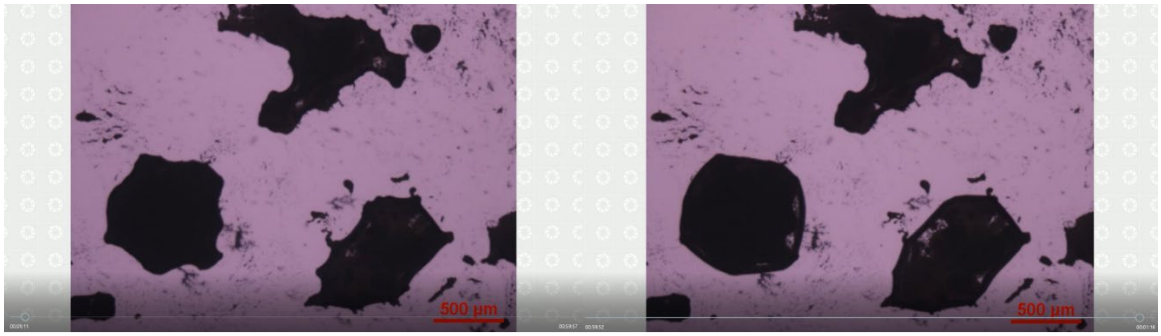

Figure 4. Time dependent appearance of pure amorphous SOR free base in water.

The marketed product Nexavar® contains micronized SOR tosylate salt, instead of the free base. To achieve higher solubility and dissolution rate, we also tried to produce SOR tosylate ASD for better *in vivo* performance. However, coprecipitation of SOR tosylate underwent disproportionation due to the high solubility of p-toluenesulfonic acid (the acid form of tosylate). The NMR peaks of the methyl group of precipitated tosylate of SOR tosylate/HPMC-AS ASD, and those of as received SOR tosylate are shown in **Figure 5**. Only 19% of tosylate precipitated because the rest was either dissolved in antisolvent during coprecipitation or was washed out by antisolvent and DI water.

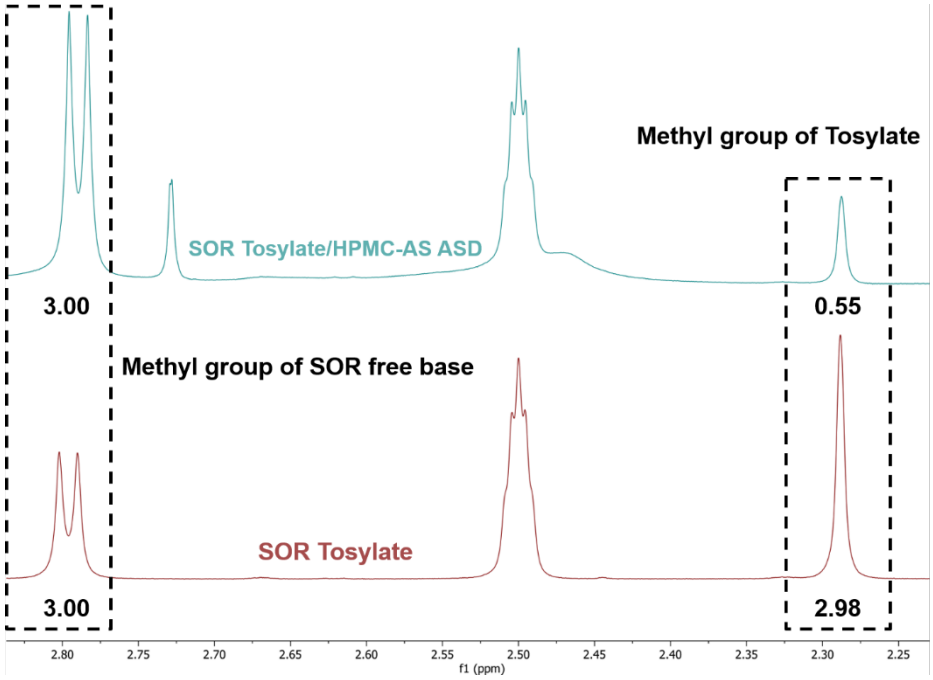

Figure 5. ^{1}H NMR of SOR Tosylate/HPMC-AS ASD and SOR Tosylate as received.

To evaluate the effect of solid form on the dissolution performance of ASD, spray dried pure amorphous SOR tosylate and SOR tosylate/HPMC-AS ASD was used (**Figure 6**). Comparison of IDR suggested a remarkable dissolution enhancement of ASDs compared to pure amorphous SOR tosylate (0.0033 µg/mL•min). The IDR of SOR free base/HPMC-AS ASD was 0.048 µg/mL•min, which was only slightly slower than that of SOR tosylate/HPMC-AS ASD, 0.068 µg/mL•min. Due to the significantly improved dissolution rate, SOR free base/HPMC-AS ASD was selected for the further tablet formulation design.

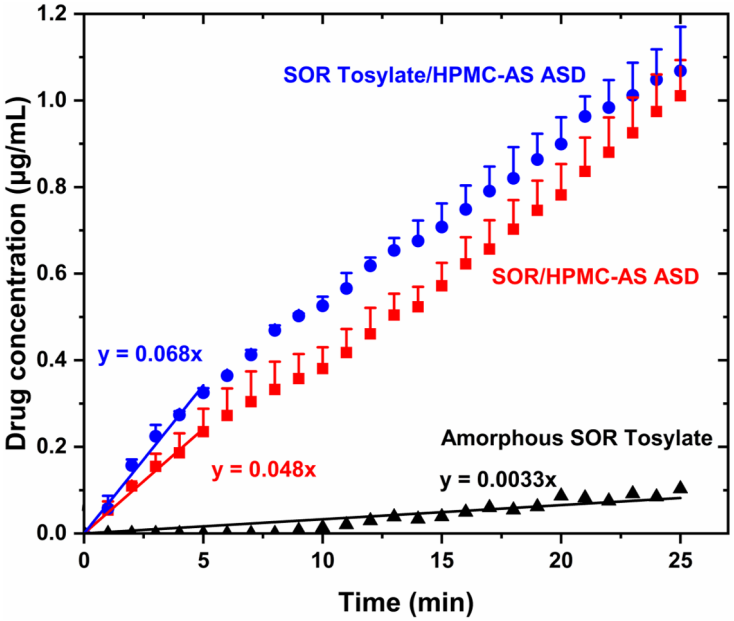

Figure 6. Intrinsic dissolution rate of SOR/HMPC-AS, SOR Tosylate/HPMC-AS ASDs and amorphous SOR tosylate.

3.2 Impact of ASD drug loading and HMPC-AS grade on drug release

HPMC-AS is a commonly used ionic polymer for oral products, because of its excellent performance in maintaining supersaturation.[24,25] Though exhibiting moderate solubility in aqueous media compared with other widely used water soluble polymers, such as polyethylene glycol (PEG), polyvinylpyrrolidone (PVP), PVP-VA, and hydroxypropyl methylcellulose (HPMC), HPMC-AS-based ASDs display shorter disintegration times and faster dissolution rates, which are largely unchanged with different drug loadings.[26] These properties are desirable for developing an immediate-release tablet. There are three commercially available grades of HPMC-AS, namely H, M, and L. Due to the different succinoyl and acetyl contents, the approximate pH values

above which each grade of HPMC-AS initially becomes ionized or soluble are 6.8 (H), 6.0 (M), and 5.5 (L).

Selection of the appropriate drug loading and grade of HPMC-AS was based on *in vitro* drug release of SOR ASDs. A common drug loading of 40% was first used to determine polymer grade. From **Figure 7A**, M grade showed the largest area under the curve (AUC) compared with the other two grades. Then, 20%, 40%, and 60 % drug loadings were tested. Of these, 60% drug loading exhibited the lowest AUC. However, there was no significant difference in AUC between 20% and 40% drug loadings (**Figure 7B**). Since higher drug loading is preferred to reduce "pill burden", 40% drug loading was chosen for subsequent studies.

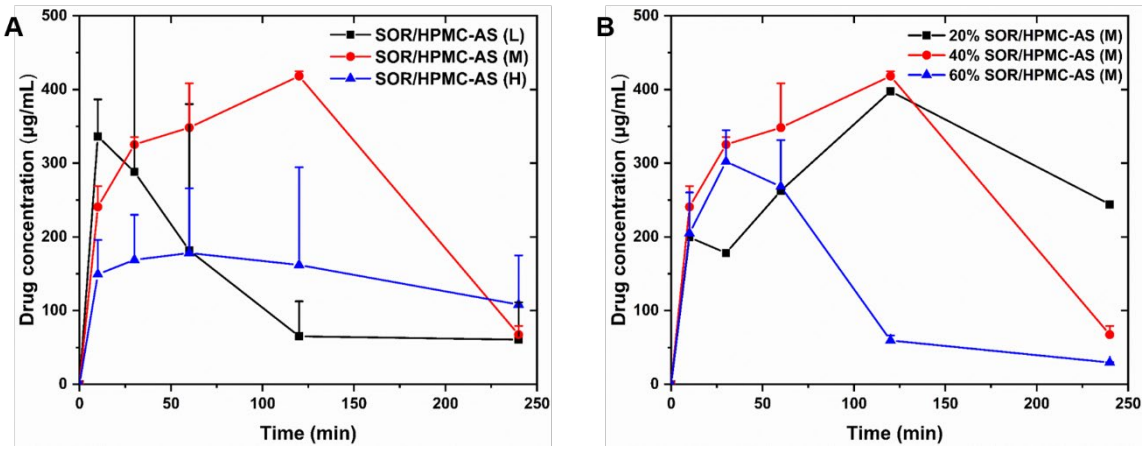

Figure 7. Powder dissolution of A) 40% drug loading SOR/HPMC-AS ASDs with L, M and H grade, B) SOR/HPMC-AS (M) ASDs with 20%, 40% and 60% drug loading.

3.3 Thermal and morphological assessment of SOR ASD

The PXRD pattern (**Figure 8A**) of SOR ASD displayed a broad halo with no characteristic Bragg diffraction peaks. Thermal analyses of crystalline SOR and SOR ASD are shown in **Figure 8B**. The T_m of SOR free base was 211.62 °C, with a heat of

fusion of 103.6 J/g. The DSC curve of the SOR ASD showed a single T_g at 94.32 °C, indicating a homogeneous single phase. There was no enthalpy relaxation endotherm observed after the glass transition event, which suggests that the drying process did not lead to a significant structural relaxation of the SOR ASD. The value of T_g was approximately 70 °C higher than room temperature. Such a temperature difference provides good physical stability [confirmed by the PLM image of stressed ASD (**Figure 9B**)], which is due to the largely reduced global mobility of homogeneous ASD, which was anti-plasticized effectively by HPMC-AS.[27-29]

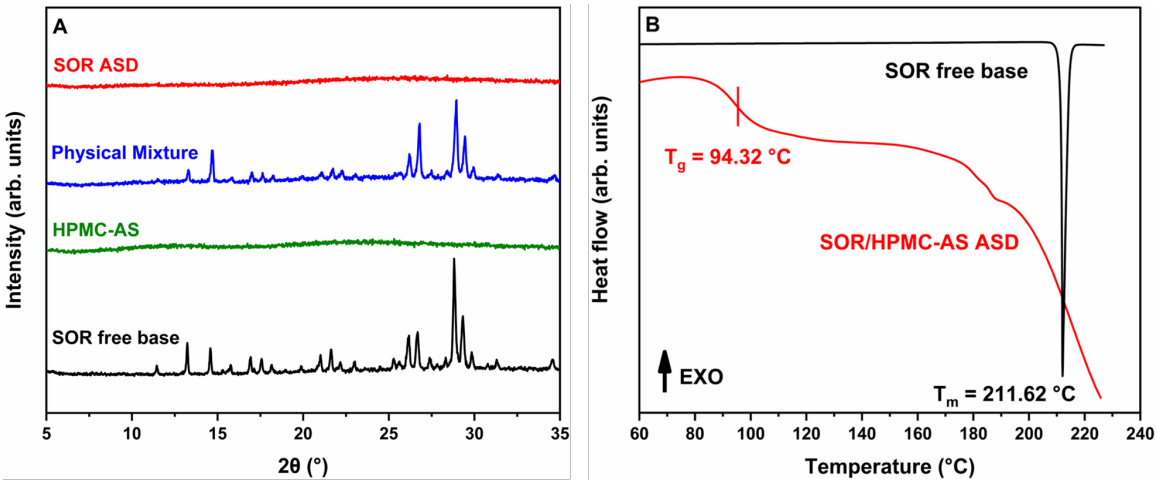

Figure 8. A) PXRD of fresh SOR ASD, physical mixture of SOR and HPMC-AS, HPMC-AS (M), and crystalline SOR free base; B) DSC of crystalline SOR free base and SOR ASD.

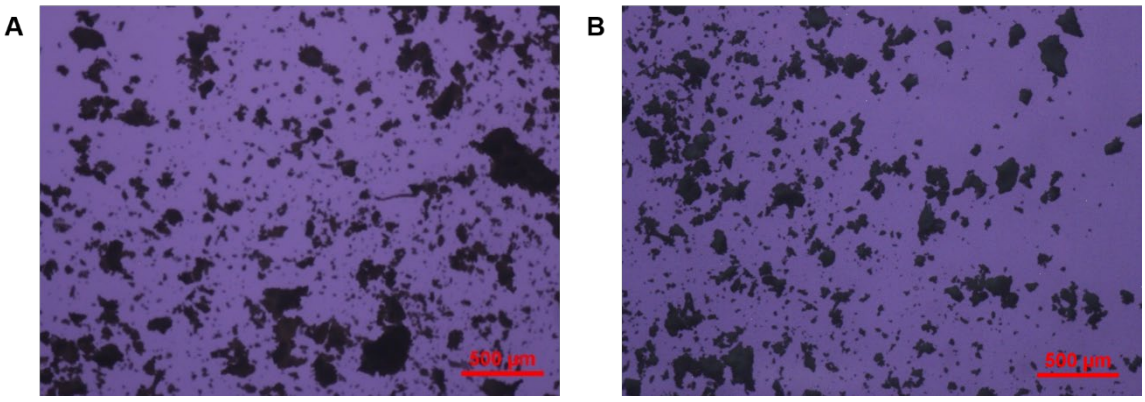

Figure 9. Images obtained by PLM. A) fresh SOR ASD, B) SOR ASD stored under stressed condition (40 °C and 57% RH) for 6 months.

The irregular morphology and highly porous microstructure of SOR ASD were captured in SEM images (**Figure 10A-B**). During the formation of coprecipitates with constant agitation, there was simultaneous diffusion of DMSO into and water out of the SOR/HPMC-AS droplets. Concurrent diffusion resulted in the coprecipitates having a "sponge-like" porous microstructure, as reported by others.[9,16]

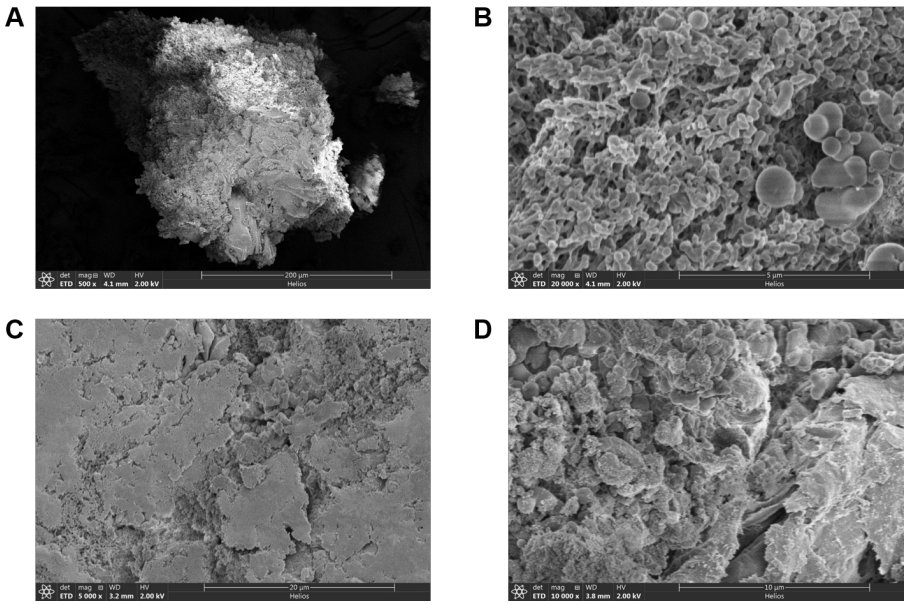

Figure 10. SEM of A-B) SOR ASD, C-D) SOR ASD tablet. Scale bars: A) 200 µm; B) 5 µm; C) 20 µm; D) 10 µm.

From vapor sorption measurements, the SOR ASD took up 3.2% moisture under 75% RH, which was less compared than that of pure HPMC-AS, 6.14% (**Figure 11**). The moderate hygroscopicity of SOR ASD partially explains its superior long term physical stability when stored under stressed conditions.[30,31]

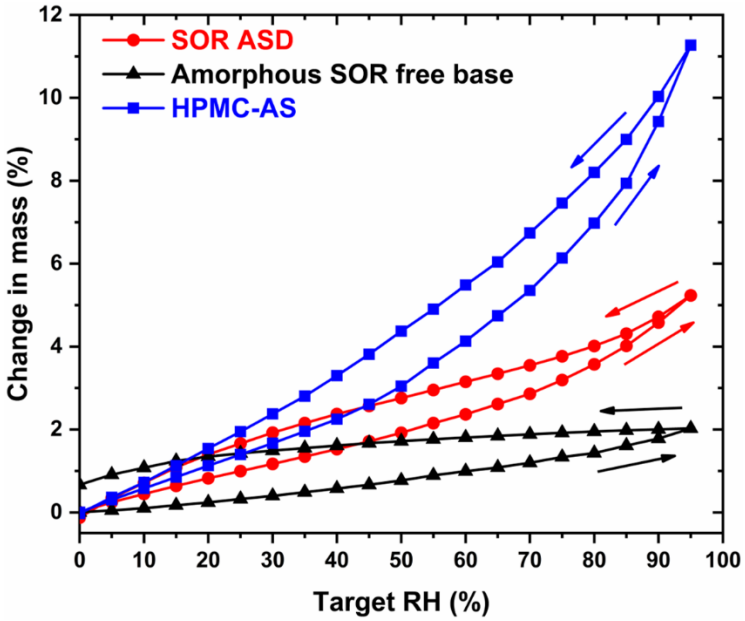

Figure 11. Vapor sorption isotherms of pure amorphous SOR free base, HPMC-AS, and SOR ASD.

3.4 Formulation optimization and tablet performance

Guided by the materials science tetrahedron principle, optimizing the process and adding functional excipients with desirable properties could overcome the deficiency of formulation performance.[32] Due to its highly porous microstructure, SOR ASD exhibited a low bulk density (0.14 ± 0.0045 g/cm^3, n=3) and poor powder flow (*ffc* = 6.13 ± 0.28, n=3). Granulation was therefore necessary for tablet manufacturing.[5,33] Because a process using water would likely adversely affect the *in vivo* performance of ASDs, dry granulation (**Figure 12**) was used.[8,34] However, dry granulation is frequently accompanied with "loss of tabletability" due to size enlargement and work hardening. Thus, a coprocessed functional excipient, Avicel® DG [75% microcrystalline cellulose and 25% dibasic calcium phosphate anhydrate (DCPA)] was selected, since DCPA is a brittle material, to maintain a balanced ductility-brittleness of the starting material.[35] The brittle

material tartaric acid was incorporated as a "disintegration facilitator". Tartaric acid can provide adequate porosity of the hydrated tablet matrix due to its high solubility in aqueous media, facilitating imbibition of water into the compact which induces swelling of crospovidone, and also serves as a pH modifier (acidifier) to facilitate solubilization of SOR in the small intestine.[36,37]

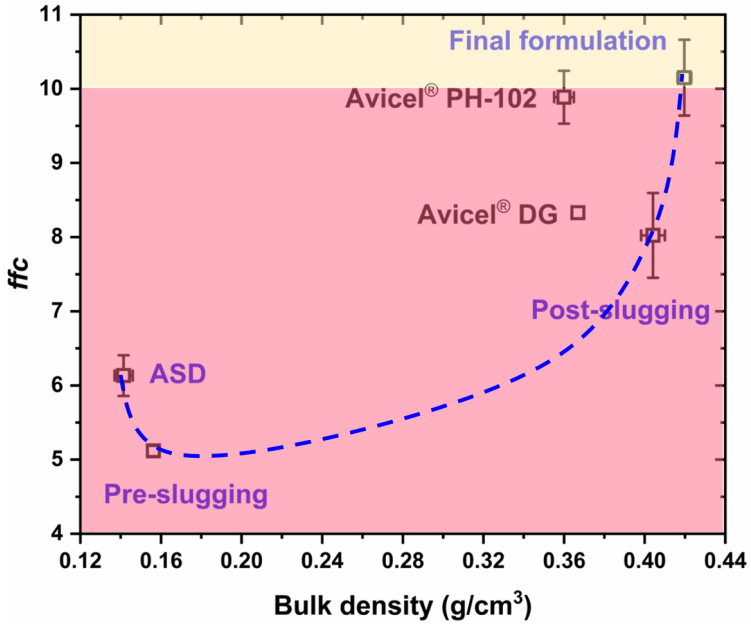

Figure 12. Formulation optimization for improved flow property and bulk density. Values of *ffc* higher than 10 indicate free-flowing powder.

It is worth noticing that the pre-slugging powder mixture (*ffc* = 5.12) displayed poorer flowability than the major constituent components (*ffc* = 9.10 for crospovidone and 12.9 for tartaric acid). The mixture was compressed under 7 KN into simulated ribbons and then ground manually. The post-slugging granules displayed a greater bulk density (0.40 ± 0.01 g/cm^3) and flow properties (*ffc* = 8.00 ± 0.57) compared to the pre-slugging powder mixture, due to densification and size enlargement.

The final formulation, containing 0.5% MgSt, exhibited both a higher bulk density (0.42 ± 0.0017 g/cm^3) and flowability (*ffc* = 10.15 ± 0.51), which is superior to the reference material Avicel® PH-102.[33,38] During tablet manufacturing, no punch sticking was observed, and the ejection force was generally lower than 100 N when simulating a high speed tableting of 74,800 tablets/hr. The final formulation could undergo plastic deformation with fast pore shrinkage and elimination (**Figure 10C-D**) under increased pressure, leading to a large bonding area, and excellent tabletability with a minimum tensile strength of 2 MPa when compression pressure was greater than around 60 MPa, as shown in **Figure 13**.[5,39]

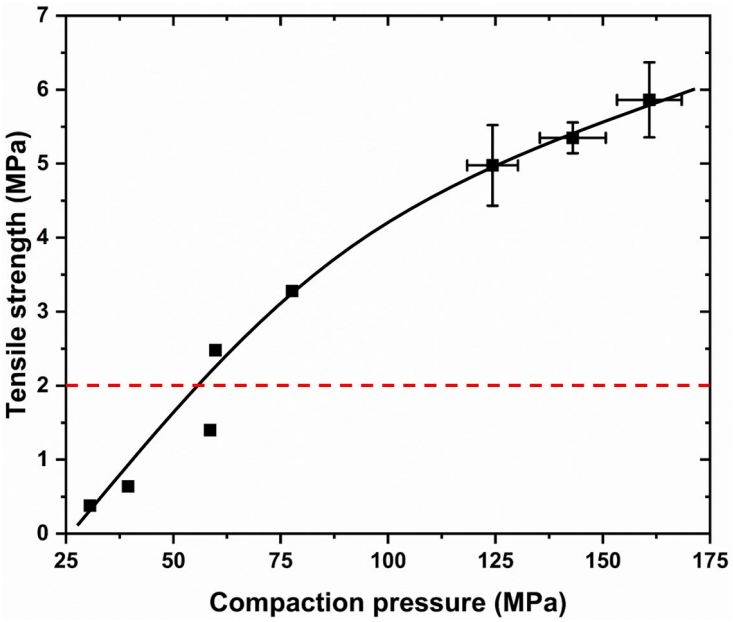

Figure 13. Tabletability of SOR ASD formulation. The dashed line of 2 MPa indicates the minimum required tablet tensile strength.

Disintegration time and friability of the tablet were investigated to optimize the compaction force for manufacturing. A force of 3 KN was selected for further studies, as a balance of low friability of ~0.04% and short disintegration time of 115 s (**Figure 14**).

Disintegration time was sensitive to compaction force. That is, with forces greater than 5 KN, tablets did not disintegrate but only underwent surface erosion in 30 min (**Figure 14** upper right corner). This could be attributed to the highly porous structure of the SOR ASD formulation (**Figure 10D**). A large compaction force may cause pore collapse, which would eliminate the path for wicking and interruption of particle-particle bonds, therefore resulting in a longer disintegration time.[40]

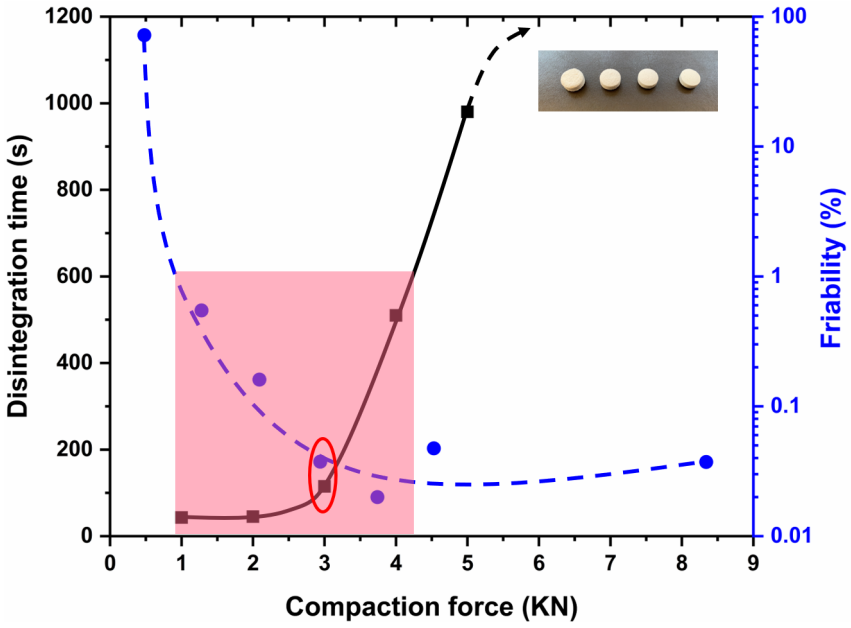

Figure 14. Compaction force optimization based on performance of friability and disintegration time. The compaction pressure range for manufacturing tablets with fast disintegration and low friability is shaded in red.

3.5 *In vitro* tablet drug release

Rapid dissolution of SOR ASD tablet containing 100 mg SOR, compared with Nexavar® containing 200 mg SOR, was achieved by adding 7% of highly soluble tartaric acid together with 5% of the superdisintegrant crospovidone. The tartaric acid dissolved quickly, rendering the tablet more porous and allowing water to penetrate rapidly by capillary action and thereby facilitate disintegration. The tartaric acid may also be effective in modifying the microenvironmental pH for enhancing drug solubility.[14] Use of the ionic polymer HPMC-AS would avoid gelation at physiological pH in the small intestine and facilitate faster dissolution compared to commonly used water soluble polymers, such as PVP, PVP-VA and HPMC.[41] HPMC-AS, which could form drug/polymer nanocolloids because of its amphiphilic structure, displayed a superior capability for supersaturation sustainment of ~28% drug release (~60 μg/mL) for the entire dissolution study of 90 min (**Figure 15**).[24] The negligible dissolution of Nexavar® during the first 10 min was attributed to the coated film on its surface. Drug release was ~5%, and the concentration of SOR during dissolution was ~20 μg/mL, slightly higher than its aqueous solubility, due to the presence of 0.1% of Tween® 80 in the dissolution media, as well as the solubilizers SLS and PEG in the formulation of Nexavar®.

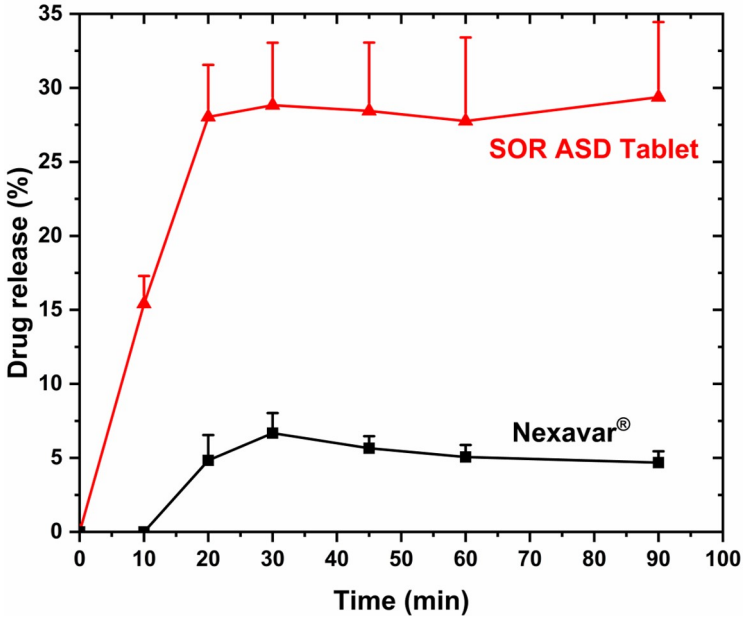

Figure 15. *In vitro* drug release (%) of SOR ASD tablet and Nexavar®.

3.6 Relative oral bioavailability of SOR ASD tablet compared with its commercial tablet Nexavar® containing SOR crystalline salt

In vivo exposure following SOR release from the ASD tablet (100 mg SOR/tablet) and the commercial product Nexavar® (200 mg SOR/tablet) was assessed in Beagle dogs, in a pilot study with n=3. The pharmacokinetics of SOR was established to be dose-independent, since the elimination rate constants (λ_z) for both SOR ASD tablet (and 0.15 ± 0.07 hr^{-1}) and Nexavar® (0.15 ± 0.05 hr^{-1}) were almost identical. Therefore, the doses of these two formulations were normalized to 100 mg/tablet for further analysis.

The plasma SOR concentration-time profiles are displayed in **Figure 16**, and the noncompartmental PK parameters are summarized in **Table 3**. Exposure ($AUC_{0\text{-inf}}$) following administration of the SOR ASD tablet was 8117.36 ± 2850.93 hr*ng/mL, which

was considerably higher than $AUC_{0\text{-}inf}$ of 5415.91 ± 1850.75 hr*ng/mL for Nexavar®. The maximum plasma concentration (C_{max}) of SOR was 813.76 ± 334.02 ng/mL for the ASD tablet, which was slightly higher than that of Nexavar®, 760.58 ± 280.88 ng/mL. The corresponding T_{max} values were 3.17 ± 1.18 hr and 1.50 ± 0.41 hr, respectively. These results, which indicate prolonged and increased absorption, are consistent with the formation of SOR/HPMC-AS nanocolloids, which exhibit good stability and prevent the conversion of SOR from the amorphous form to its crystalline counterpart in the small intestine.[24]

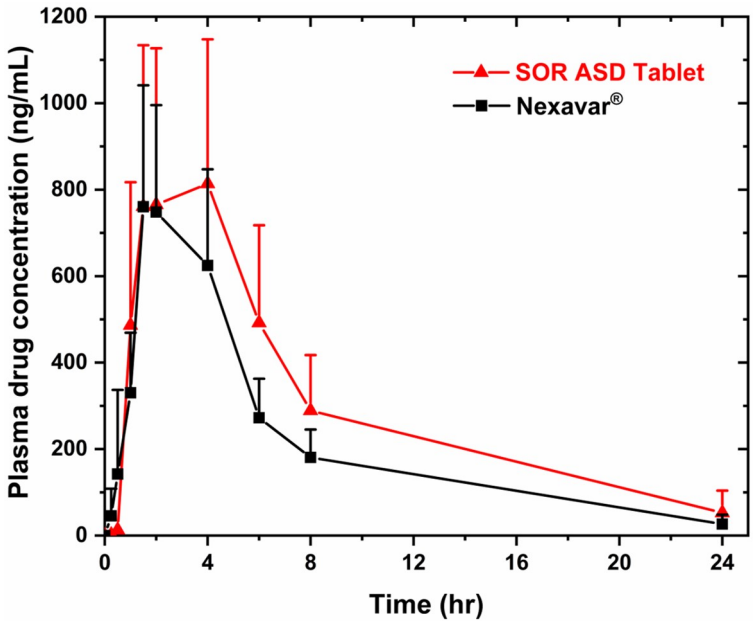

Figure 16. *In vivo* pharmacokinetic study of SOR ASD tablet and Nexavar® (Dose normalized to 100 mg/Tablet).

Table 3. Non-compartmental PK parameters (Mean ± SD, n = 3) of SOR ASD tablet and Nexavar® (Dose normalized to 100 mg/Tablet).

Parameter	Nexavar®	SOR ASD Tablet
C_{max} (ng/mL)	760.58 ± 280.88	813.76 ± 334.02
T_{max} (hr)	1.50 ± 0.41	3.17 ± 1.18
$AUC_{0\text{-}24}$ (hr*ng/mL)	5177.11 ± 1639.91	7216.04 ± 2965.21
$AUC_{0\text{-}inf}$ (hr*ng/mL)	5415.91 ± 1850.75	8117.36 ± 2850.93
λ_z (hr^{-1})	0.15 ± 0.05	0.15 ± 0.07
Relative oral bioavailability	1.00	1.50 ± 0.028

While the sample size in this pilot study is too small to draw definitive conclusions regarding absorption enhancement, we consider it worthwhile to determine, for each individual dog, the relative oral bioavailability. In **Table 4** we list dose normalized $AUC_{0\text{-}inf}$ values for Nexavar® and for the SOR ASD tablet, and take their ratios, which provides an estimate of relative oral bioavailabilities for each dog. These relative bioavailability estimates cluster tightly around 1.5, even though there are rather large intersubject variabilities in the $AUC_{0\text{-}inf}$ values. Thus, this small pilot study suggests an increase in oral bioavailability of ~50%.

Table 4. $AUC_{0\text{-}inf}$ of Nexavar® and SOR ASD tablet, relative oral bioavailability of each of 3 dogs (Dose normalized to 100 mg/Tablet).

	Dog 1	Dog 2	Dog 3
$AUC_{0\text{-}inf}$ of Nexavar® (hr*ng/mL)	5754.64	7494.17	2998.91
$AUC_{0\text{-}inf}$ of SOR ASD tablet (hr*ng/mL)	8405.58	11455.98	4490.57
Relative oral bioavailability	1.46	1.53	1.50

Although the correct rank order of *in vitro* and *in vivo* performance of SOR ASD tablet and Nexavar® was established, the enhancement of relative oral bioavailability of SOR ASD tablet was less than the vastly increased drug release *in vitro*. Several cases of ASDs were reported that they could not show an *in vitro – in vivo* linear relation, which could be ascribed to the overestimation of *in vitro* dissolution enhancement, due to the different composition and volume between artificial dissolution medium and gastrointestinal fluid, as well as their different hydrodynamics.[3,42] For the *in vitro* dissolution study, a large volume of the medium (500 mL) and vigorous agitation (paddle rotating at 75 rpm) was applied. These conditions guaranteed rapid dissolution *in vitro*. However, the volumes of stomach and small intestine fluids of the dogs were small (~20 and 300 mL in fasted state, respectively), and peristalsis was slow, which may have led to slower disintegration and dissolution *in vivo*.[13,43-45]

4. Conclusions

We have prepared SOR ASD *via* coprecipitation with the polymer, HPMC-AS. The SOR ASD showed excellent physical stability and improved intrinsic dissolution rate, which is favorable for the formulation development of such BCS II drugs. The drug loadings and polymer grades were further assessed to facilitate ASD tablet development. The formulation composition and processes were designed based on the materials science tetrahedron principle. The manufacturing compaction pressure was optimized based on the balance of the tablet disintegration time and friability. The resulting ASD tablets displayed a faster rate and superior extent of *in vitro* dissolution, as well as 50% enhancement of the relative oral bioavailability compared with the commercial product, Nexavar®. It was demonstrated that such a material sparing and expedited approach is effective for ASD tablet formulation development.

Bibliography

1. Pouton CW 2006. Formulation of poorly water-soluble drugs for oral administration: Physicochemical and physiological issues and the lipid formulation classification system. Eur J Pharm Sci 29(3):278-287.

2. Amidon GL, Lennernäs H, Shah VP, Crison JR 1995. A Theoretical Basis for a Biopharmaceutic Drug Classification: The Correlation of in Vitro Drug Product Dissolution and in Vivo Bioavailability. Pharm Res 12(3):413-420.

3. Newman A, Knipp G, Zografi G 2012. Assessing the performance of amorphous solid dispersions. J Pharm Sci 101(4):1355-1377.

4. Jermain SV, Brough C, Williams RO 2018. Amorphous solid dispersions and nanocrystal technologies for poorly water-soluble drug delivery – An update. Int J Pharm 535(1):379-392.

5. Serajuddin ATM 1999. Solid dispersion of poorly water-soluble drugs: Early promises, subsequent problems, and recent breakthroughs. J Pharm Sci 88(10):1058-1066.

6. Singh A, Van den Mooter G 2016. Spray drying formulation of amorphous solid dispersions. Adv Drug Deliv Rev 100:27-50.

7. Patil H, Tiwari RV, Repka MA 2016. Hot-Melt Extrusion: from Theory to Application in Pharmaceutical Formulation. AAPS PharmSciTech 17(1):20-42.

8. Hu Q, Choi DS, Chokshi H, Shah N, Sandhu H 2013. Highly efficient miniaturized coprecipitation screening (MiCoS) for amorphous solid dispersion formulation development. Int J Pharm 450(1):53-62.

9. Shah N, Sandhu H, Choi DS, Chokshi H, Malick AW. 2014. Amorphous Solid Dispersions: Theory and Practice. ed.: Springer New York.

10. Shah N, Sandhu H, Phuapradit W, Pinal R, Iyer R, Albano A, Chatterji A, Anand S, Choi DS, Tang K, Tian H, Chokshi H, Singhal D, Malick W 2012. Development of novel microprecipitated bulk powder (MBP) technology for manufacturing stable amorphous formulations of poorly soluble drugs. Int J Pharm 438(1):53-60.

11. Wilhelm S, Carter C, Lynch M, Lowinger T, Dumas J, Smith RA, Schwartz B, Simantov R, Kelley S 2006. Discovery and development of sorafenib: a multikinase inhibitor for treating cancer. Nat Rev Drug Discov 5(10):835-844.

12. Llovet JM, Ricci S, Mazzaferro V, Hilgard P, Gane E, Blanc J-F, de Oliveira AC, Santoro A, Raoul J-L, Forner A, Schwartz M, Porta C, Zeuzem S, Bolondi L, Greten TF, Galle PR, Seitz J-F, Borbath I, Häussinger D, Giannaris T, Shan M, Moscovici M, Voliotis D, Bruix J 2008. Sorafenib in Advanced Hepatocellular Carcinoma. N Engl J Med 359(4):378-390.

13. Almeida e Sousa L, Reutzel-Edens SM, Stephenson GA, Taylor LS 2015. Assessment of the Amorphous "Solubility" of a Group of Diverse Drugs Using New Experimental and Theoretical Approaches. Mol Pharm 12(2):484-495.

14. Liu C, Chen Z, Chen Y, Lu J, Li Y, Wang S, Wu G, Qian F 2016. Improving Oral Bioavailability of Sorafenib by Optimizing the "Spring" and "Parachute" Based on Molecular Interaction Mechanisms. Mol Pharm 13(2):599-608.

15. Shi Y, Zhao Z, Gao Y, Pan DC, Salinas AK, Tanner EEL, Guo J, Mitragotri S 2020. Oral delivery of sorafenib through spontaneous formation of ionic liquid nanocomplexes. J Control Release 322:602-609.

16. Park SY, Kang Z, Thapa P, Jin YS, Park JW, Lim HJ, Lee JY, Lee S-W, Seo M-H, Kim M-S, Jeong SH 2019. Development of sorafenib loaded nanoparticles to improve oral bioavailability using a quality by design approach. Int J Pharm 566:229-238.

17. Wang X-q, Fan J-m, Liu Y-o, Zhao B, Jia Z-r, Zhang Q 2011. Bioavailability and pharmacokinetics of sorafenib suspension, nanoparticles and nanomatrix for oral administration to rat. Int J Pharm 419(1):339-346.

18. Zhang Z, Niu B, Chen J, He X, Bao X, Zhu J, Yu H, Li Y 2014. The use of lipid-coated nanodiamond to improve bioavailability and efficacy of sorafenib in resisting metastasis of gastric cancer. Biomaterials 35(15):4565-4572.

19. Ya-Ou Liu J-MFX-QWQZ 2011. Preparation of sorafenib self-microemulsifying drug delivery system and its relative bioavailability in rats. J Chin Pharm Sci 20(2):164-170.

20. Park J-H, Baek M-J, Lee J-Y, Kim K-T, Cho H-J, Kim D-D 2020. Preparation and characterization of sorafenib-loaded microprecipitated bulk powder for enhancing oral bioavailability. Int J Pharm 589:119836.

21. Schulze D. 2007. Powders and Bulk Solids: Behavior, Characterization, Storage and Flow. ed.: Springer Berlin Heidelberg.

22. Fell JT, Newton JM 1970. Determination of Tablet Strength by the Diametral-Compression Test. J Pharm Sci 59(5):688-691.

23. Osei-Yeboah F, Sun CC 2015. Validation and applications of an expedited tablet friability method. Int J Pharm 484(1):146-155.

24. Friesen DT, Shanker R, Crew M, Smithey DT, Curatolo WJ, Nightingale JAS 2008. Hydroxypropyl Methylcellulose Acetate Succinate-Based Spray-Dried Dispersions: An Overview. Mol Pharm 5(6):1003-1019.

25. Curatolo W, Nightingale JA, Herbig SM 2009. Utility of Hydroxypropylmethylcellulose Acetate Succinate (HPMCAS) for Initiation and Maintenance of Drug Supersaturation in the GI Milieu. Pharm Res 26(6):1419-1431.

26. Zhang W, Noland R, Chin S, Petkovic M, Zuniga R, Santarra B, Conklin B, Hou HH, Nagapudi K, Gruenhagen JA, Yehl P, Chen T 2021. Impact of polymer type, ASD loading and polymer-drug ratio on ASD tablet disintegration and drug release. Int J Pharm 592:120087.

27. Yu L 2001. Amorphous pharmaceutical solids: preparation, characterization and stabilization. Adv Drug Deliv Rev 48(1):27-42.

28. Hancock BC, Shamblin SL, Zografi G 1995. Molecular Mobility of Amorphous Pharmaceutical Solids Below Their Glass Transition Temperatures. Pharm Res 12(6):799-806.

29. Zografi G, Newman A 2017. Interrelationships Between Structure and the Properties of Amorphous Solids of Pharmaceutical Interest. J Pharm Sci 106(1):5-27.

30. Ahlneck C, Zografi G 1990. The molecular basis of moisture effects on the physical and chemical stability of drugs in the solid state. Int J Pharm 62(2):87-95.

31. Newman AW, Reutzel‐Edens SM, Zografi G 2008. Characterization of the "hygroscopic" properties of active pharmaceutical ingredients. J Pharm Sci 97(3):1047-1059.

32. Sun CC 2009. Materials Science Tetrahedron—A Useful Tool for Pharmaceutical Research and Development. J Pharm Sci 98(5):1671-1687.

33. Sun CC 2010. Setting the bar for powder flow properties in successful high speed tableting. Powder Technol 201(1):106-108.

34. Démuth B, Nagy ZK, Balogh A, Vigh T, Marosi G, Verreck G, Van Assche I, Brewster ME 2015. Downstream processing of polymer-based amorphous solid dispersions to generate tablet formulations. Int J Pharm 486(1):268-286.

35. Sun CC, Kleinebudde P 2016. Mini review: Mechanisms to the loss of tabletability by dry granulation. Eur J Pharm Biopharm 106:9-14.

36. Tran PH-L, Tran TT-D, Lee K-H, Kim D-J, Lee B-J 2010. Dissolution-modulating mechanism of pH modifiers in solid dispersion containing weakly acidic or basic drugs with poor water solubility. Expert Opin Drug Deliv 7(5):647-661.

37. Desai PM, Liew CV, Heng PWS 2016. Review of Disintegrants and the Disintegration Phenomena. J Pharm Sci 105(9):2545-2555.

38. Wei G, Mangal S, Denman J, Gengenbach T, Lee Bonar K, Khan RI, Qu L, Li T, Zhou Q 2017. Effects of Coating Materials and Processing Conditions on Flow Enhancement of Cohesive Acetaminophen Powders by High-Shear Processing With Pharmaceutical Lubricants. J Pharm Sci 106(10):3022-3032.

39. Hou HH, Rajesh A, Pandya KM, Lubach JW, Muliadi A, Yost E, Jia W, Nagapudi K 2019. Impact of Method of Preparation of Amorphous Solid Dispersions on Mechanical Properties: Comparison of Coprecipitation and Spray Drying. J Pharm Sci 108(2):870-879.

40. Markl D, Zeitler JA 2017. A Review of Disintegration Mechanisms and Measurement Techniques. Pharm Res 34(5):890-917.

41. Mudie DM, Buchanan S, Stewart AM, Smith A, Shepard KB, Biswas N, Marshall D, Ekdahl A, Pluntze A, Craig CD, Morgen MM, Baumann JM, Vodak DT 2020. A novel architecture for achieving high drug loading in amorphous spray dried dispersion tablets. Int J Pharm: X 2:100042.

42. Mudie DM, Stewart AM, Biswas N, Brodeur TJ, Shepard KB, Smith A, Morgen MM, Baumann JM, Vodak DT 2020. Novel High-Drug-Loaded Amorphous Dispersion Tablets of Posaconazole; In Vivo and In Vitro Assessment. Mol Pharm 17(12):4463-4472.

43. Hatton GB, Yadav V, Basit AW, Merchant HA 2015. Animal Farm: Considerations in Animal Gastrointestinal Physiology and Relevance to Drug Delivery in Humans. J Pharm Sci 104(9):2747-2776.

44. Liu C, Liu Z, Chen Y, Chen Z, Chen H, Pui Y, Qian F 2018. Oral bioavailability enhancement of β-lapachone, a poorly soluble fast crystallizer, by cocrystal, amorphous solid dispersion, and crystalline solid dispersion. Eur J Pharm Biopharm 124:73-81.

45. Dressman JB 1986. Comparison of Canine and Human Gastrointestinal Physiology. Pharm Res 3(3):123-131.